International Journal of Engineering & Technology, 7 (2.24) (2018) 283-290

International Journal of Engineering & Technology

Website: www.sciencepubco.com/index.php/IJET

Research paper

Adaptive Fuzzy Controller Design for Solar And Wind Based Hybrid System

M.Rathaiah[1], P.Ram Kishore Kumar Reddy[2], P.Sujatha[3]

[1]Research Scholar, Department of Electrical Engineering, JNTUA, Ananthapuramu
[2]Professor,Department of Electrical EngineeringMGIT, Hyderabad
[3]Professor,Department of Electrical Engineering,JNTUACEA, Ananthapuramu

Abstract

Renewable Energy Resources plays an active role in standing against global warming and reduce the use of conventional energy sources. Hybrid systems formed by combining the renewable energy sources are efficient relatively. The intent of this paper is to furnish endurable power for frontier and far-off places with hybrid-system of architecture. The intended system embodying DFIG and solar PV based wind turbine. In solar systems, control mechanism is essential for improving the performance. This paper proposes a method of incremental conductance approach based MPPT Adaptive Fuzzy Logic Controller for grid connected PV system which is composed of a boost converter and a three phase inverter. Adaptive Fuzzy Logic Controller provides fast response and better %THD compared to Fuzzy and PI controllers. In solar system, MPPT will magnify solar output power value. The DFIG has two controllers Grid-Side Control (GSC) and Rotor-Side Control (RSC). The rated rotor speed and DC-link voltage are regulated by RSC and GSC through PI, Fuzzy Logic Controller and AFLC strategies. By using simulation studies performed by three control strategies, %THD analysis is carried out.

Keywords: *PV panel, Double –Fed –Induction Generator (DFIG), Wind Energy Conversion System (WECS), Rotor Side Control (RSC), Grid Side Control (GSC), AFLC, %THD.*

1. Introduction

Because of exhaustion of the fossil fuel and pollution, renewable energy utilities have been developed recently. The diminutiveness discrete wind power systems with a battery bank as an storage integrant is prevalent and it is imperative to a firm and endurable power in rural and remote areas [1].
The solar and wind energy are irregular and unreliable which are the main drawbacks. By combining both, steadfastness of system can be intensified. Efficient energy can be generated by using combination of energy sources. Hybrid-energy systems (HES) have more ambit in frontier and far-off areas as they cannot get supply from the grid. Renewable energy sources are preferable due to increased demand and diminution of conventional energy sources. Though there are many hybrid systems, solar and wind energy gives better results among them [2]. As solar energy is pollution free, cost effective and readily available source, it is considered as the best among the all renewable energy sources.
Wind energy is hugely available in rural areas. For larger scale power generation [5], DFIG based Wind turbine is used. The mainstream high-power WECS uses DFIG. The back- to- back converters are RSC and GSC which are connected back-to-back. In order to keep the voltage variation in the dc-link [6].The main advantages are reduced power rating, less cost, less power loss and improved efficiency. In this work, A mamdani model based FLC is contrived in the place of PI controller to control DFIG [7]. Controllers for non-linear systems [13-18].

2. Proposed System

The block diagram of the proposed system is shown in fig.1.

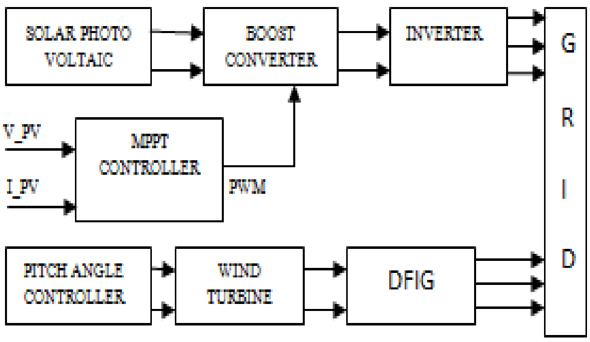

Fig.1: Block Diagram for the proposed system

2.1. Mathematical model

The equivalent circuit of a solar cell is shown in fig.2. By using photovoltaic effect, the light energy of the sun is directly converted to electricity in PV system. By using the temperature and irradiance, the PV cell current is controlled. If the irradiation is high, then the current produced is also high. A current source with a parallel diode [2], [6] is taken as model of an ideal solar cell. Any practical system has some losses and to represent these losses we use series resistance (R_s) of small value and a shunt resistance (R_P) of high value.

$$I = I_l - (I_0\left[e\left(V + {IR_s}/{V_T}\right) - 1\right] - \left(V + {IR_s}/{R_p}\right)) \quad (1)$$

here

I_l : Light generated current

I_o : Reverse saturation current

V_T : Thermal voltage

V : Solar cell voltage

I : Solar cell current

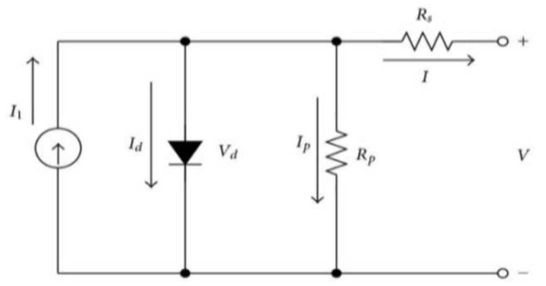

Fig. 2: One diode model of solar cell.

2.2. MPPT Evaluation algorithm

The major importance in PV system is given to the operation of system at MPP. Steps are

1: The outputs are taken from solar panel and are given to MPPT controller.

2: The present, past V & I values are dissected and provides $\Delta V = V_{new} - V_{old}$, $\Delta I = I_{new} - I_{old}$

3: The tracing of MPP is calculated by $\Delta I/\Delta V$ gradient.

4: The error is obtained by adding InCond di/dv and instant cond i/v which is e= i/v + di/dv.

5: This error is given to PI controller which minimizes its value e to zero.

6: The duty ratio is produced by PI controller .It is used to produce PWM pulses by giving it to comparators and these pulses are given to boost converter for switching purpose.

7: All the above steps are repeated until the system reaches MPP.

2.3 DC-DC Boost Converter

The Boost Converter is a step up DC-DC converter and BJT, MOSFET, TGBT etc.., are the switches used. To maintain constant output voltage the switching pulses are given by MPPT controller.

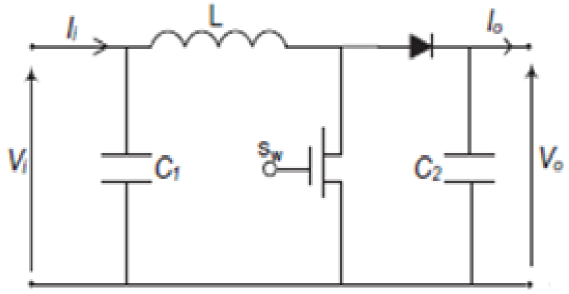

Fig. 3: Block diagram of Boost converter

Table 1: Parameters used in modeling the simulation system

(a)Parameters of Solar panel

Parameter	Value
Maximum power	3000W
Voltage V_{max}	300V
Current I_{max}	8.9A
V_{oc}	37.3V
I_{sc}	8.71A

(b)Parameters of grid

Parameter	Value
Grid voltage(V_{rms})	33kv
Grid current	4A
Grid frequency	50 Hz

3. Wind Turbine modeling

In this modeling, wind turbine transforms wind's kinetic energy into mechanical energy. Based on this, the following correlations are used for modeling. The output power of the wind turbine is given by eq [9].

$$P_m = \frac{1}{2} C_p(\lambda,\ \beta)\rho A \mathrm{v}^3 \quad (2)$$

here, ρ is the air density, v is wind speed.

The normalized form of eq(2) in P.U system is:

$$P_m(pu) = k_p C_p \mathrm{v}^3 \quad (3)$$

A generic eq is used to model $c_p(\lambda, \beta)$.

$$c_p(\lambda, \beta) = c_1\left({c_2}/{\lambda_i} - c_3\beta - c_4\right)e^{-c5/\lambda_i + c_6\lambda} \quad (4)$$

Where,

$$\frac{1}{\lambda_i} = \frac{1}{\lambda + 0.08\beta} - \frac{0.035}{\beta^3 + 1}$$

The three inputs are the generator speed in pu , pitch angle β in degrees and wind speed in m/s. The output is torque in Nm.

4. Modeling of DFIG

The equations DFIG in dq reference frame are[10]:

$$V_{qs} = R_s I_{qs} + \frac{d\emptyset_{qs}}{dt} + \omega_e \emptyset_{ds} \quad (5)$$

$$V_{ds} = R_s I_{ds} + \frac{d\emptyset_{ds}}{dt} - \omega_e \emptyset_{qs} \quad (6)$$

$$V_{dr} = R_r I_{dr} + \frac{d\emptyset_{dr}}{dt} - (\omega_e - \omega_r)\emptyset_{qr} \quad (7)$$

$$V_{qr} = R_r I_{qr} + \frac{d\emptyset_{qr}}{dt} - (\omega_e - \omega_r)\emptyset_{dr} \quad (8)$$

$$\emptyset_{ds} = L_{ls} I_{ds} + L_m(I_{ds} + I_{dr}) \quad (9)$$

$$\emptyset_{qs} = L_{ls} I_{qs} + L_m(I_{qs} + I_{qr}) \quad (10)$$

$$\emptyset_{qr} = L_{lr} I_{qr} + L_m(I_{qs} + I_{qr}) \quad (11)$$

$$\emptyset_{dr} = L_{lr} I_{dr} + L_m(I_{ds} + I_{dr}) \quad (12)$$

4.1 Rotor side controller

Vector control principle is used in this scheme.

$$I_{qr} = -\frac{L_s}{L_m} I_{qs} \quad (13)$$

Similarly I_{dr} is written in terms of I_{ds} and $\emptyset_{ds}$

$$I_{dr} = -\frac{L_s}{L_m} I_{ds} + \frac{1}{L_m}\emptyset_{ds} \quad (14)$$

From DFIG modeling

$$\emptyset_{qr} = L_{lr} I_{qr} + L_m(I_{qs} + I_{qr})$$

$$\emptyset_{dr} = L_{lr} I_{dr} + L_m(I_{ds} + I_{dr})$$

Substituting the values of I_{dr} and I_{qr} in the above equation.

$$\emptyset_{dr} = L_r \sigma I_{dr} + \frac{L_m}{L_s}\emptyset_{ds} \quad (15)$$

$$\emptyset_{qr} = \sigma L_r I_{qr} \quad (16)$$

$$V_{qr} = R_r I_{qr} + (\omega_e - \omega_r)\sigma L_r I_{dr} + \sigma L_r \frac{dI_{qr}}{dt} + (\omega_e - \omega_r)\frac{L_m}{L_s}\emptyset_{ds} \quad (17)$$

$$V_{dr} = R_r I_{dr} - (\omega_e - \omega_r)\sigma L_r I_{qr} + \sigma L_r \frac{dI_{dr}}{dt} + \frac{L_m}{L_s}\frac{d\emptyset_{ds}}{dt} \quad (18)$$

Control eq (17) and (18) are expressed with compensating terms as

$$V_{dr} = (k_{p3} + k_{i3})(I_{dr}^{*} - I_{dr}) - (\omega_e - \omega_r)L_r I_{qr} \quad (19)$$

$$V_{qr} = (k_{p4} + k_{i4})(I_{qr}^{*} - I_{qr}) + (\omega_e - \omega_r)L_r I_{dr} + (\omega_e - \omega_r)\frac{L_m}{L_s}\emptyset_{ds} \quad (20)$$

4.2 Grid Side Controller

DC-link capacitor can be expressed as:

$$C\frac{dV_{dc}}{dt} = i_{os} - i_{or} \quad (21)$$

Aligning the d-axis of the reference frame along the stator-voltage position i.e V_q=0.

$$v_{d1} = -\left(RI_d + L\frac{dI_d}{dt}\right) + \omega_e L I_q + v_d \quad (22)$$

$$v_{q1} = -\left(RI_q + L\frac{dI_q}{dt}\right) - \omega_e L I_d \quad (23)$$

The controller eq of the grid-side converters are:

$$v^{*}{}_{q1} = -(k_{p2} + k_{i2})(I^{*}{}_{q} - I_q) + \omega_e L I_d + v_q \quad (24)$$

$$v^{*}{}_{d1} = -(k_{p1} + k_{i1})(I^{*}{}_{d} - I_d) + \omega_e L I_q + v_d \quad (25)$$

4.3 Pitch angle controller

To accelerate turbine faster, restrict the rated power at high and low wind conditions and for that Pitch angle controller is required. To retain esteem value, pitch control come into picture and the speed of generator overreach rated speed. W^{ref}=1pu.

$$\frac{d\beta}{dt} = \frac{-(\beta_{ref} - \beta)}{T\beta} \quad (26)$$

Where,
β is the pitch angle

5. Control strategies

5.1 PI Controller

It is widely used for wind turbine control applications. PI controller involves the proportional gainK_p and integral gainK_i. The error signal goes to PI control loop where it gets multiplied by the proportional constant (K_p) and integral constant (K_i).

For a PI controller,

$$G_c(s) = K_p + \frac{K_i}{s} \quad (27)$$

Where
K_p= Proportional gain
K_i= integral gain

5.2 Fuzzy Logic Controller

FLC is a control method where linguistic variables are used to govern the circuit rather than mathematical values. This method is more robust than the classical controllers and can work with less data [11].
Here the membership function considered, is triangular.The membership function values are separated into seven sets and they are named as: Positive Big (PB), Zero (ZE), Negative Small (NS), Positive Small (PS), Negative Medium (NM) and Positive Medium (PM), Negative Big (NB).The controller outputΔD_N, I_d^{*} andI_{qr}^{*} for a FLC depends on the fuzzy rules shown in table.2.
The inference method used is mamdani method. The defuzzification method used is centre of area method.

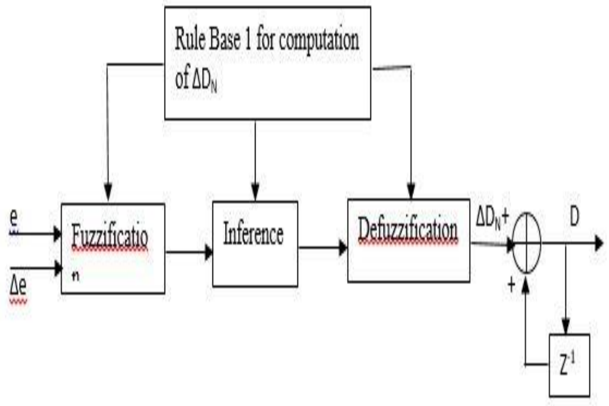

Fig. 4: Fuzzy Logic Controller structure for solar system

From above fig.4. 'e' is the error, sum of instant and Inc conductance. The controller output ΔD_N

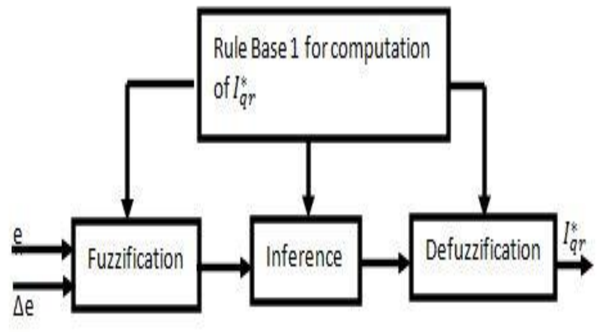

Fig. 5: Fuzzy Logic Controller structure for RSC

From the Fig.5. 'e' is the error between reference rotor angular speed and the actual rotor angular speed, the output is quadrature axis current.

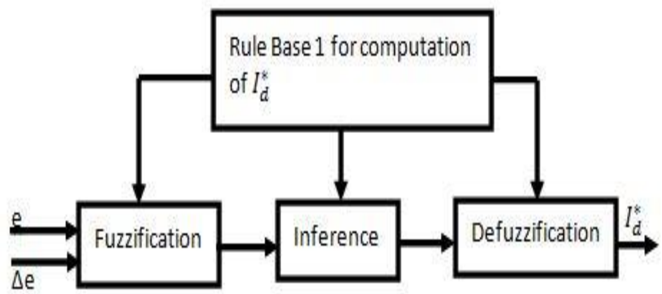

Fig. 6: Fuzzy Logic Controller structure for GSC

From the Fig.6. 'e' is error, output is the direct axis current

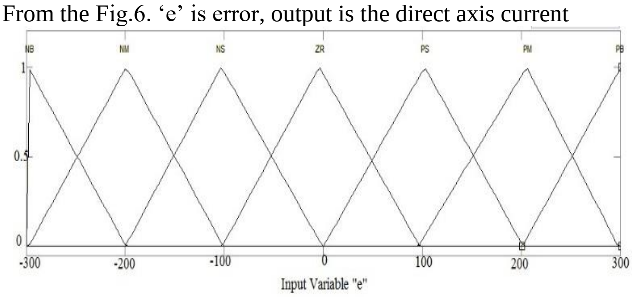

(a)

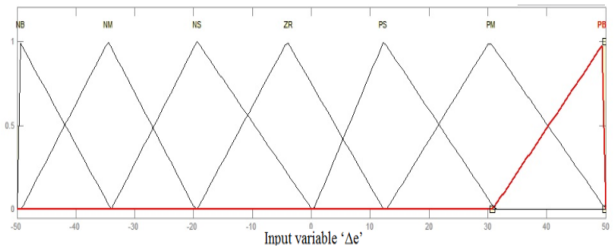

(b)

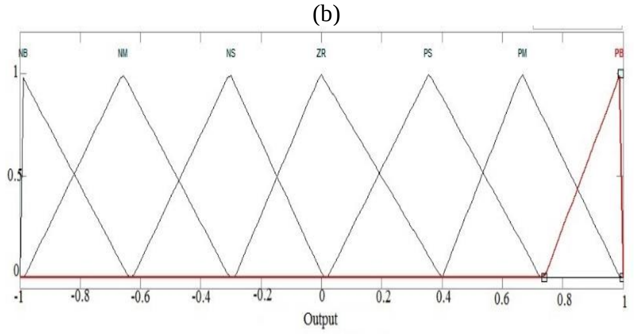

(c)

Fig. 7: MF'S of fuzzy for:(a) e(b)Δe and (c) output

Table 2: Rule base for computation of ΔD_N ,I_d^* and I_{qr}^*

e / Δe	NB	NM	NS	ZR	PS	PM	PB
NB	NB	NB	NB	NM	NM	NS	ZR
NM	NB	NB	NM	NM	NS	ZR	PS
NS	NB	NM	NM	NS	ZR	PS	PM
ZR	NM	NM	NS	ZR	PS	PM	PM
PS	NM	NS	ZR	PS	PM	PM	PB
PM	NS	ZR	PS	PM	PM	PB	PB
PB	ZR	PS	PM	PM	PB	PB	PB

5.3. Adaptive fuzzy Logic Controller

The AFLC basically consists of two fuzzy logic controllers which are connected in parallel and the corresponding block diagram shown in Fig.8, Fig.9, and Fig.10.The AFLC input and output membership functions are shown in Fig.11.

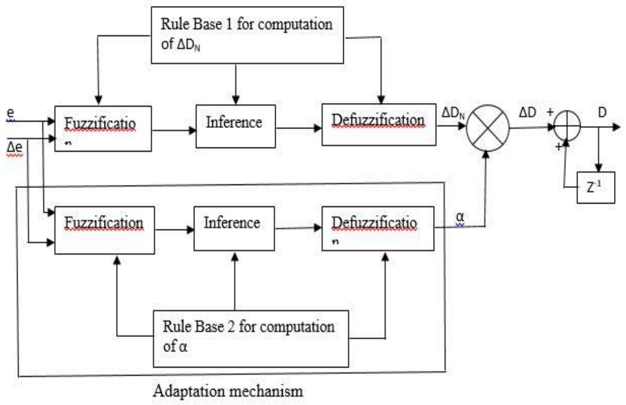

Fig.8: AFLC Structure for solar system

In this case, the incremental change in controller output ΔD is given by

$\Delta D(k)$={α(k) × $\Delta D_N(k)$}

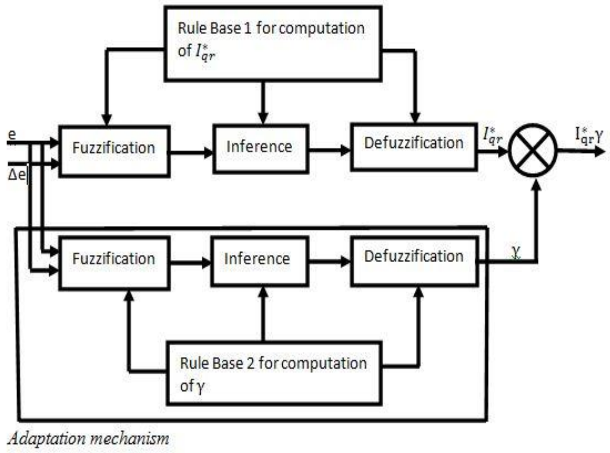

Fig. 9: AFLC Structure for RSC.

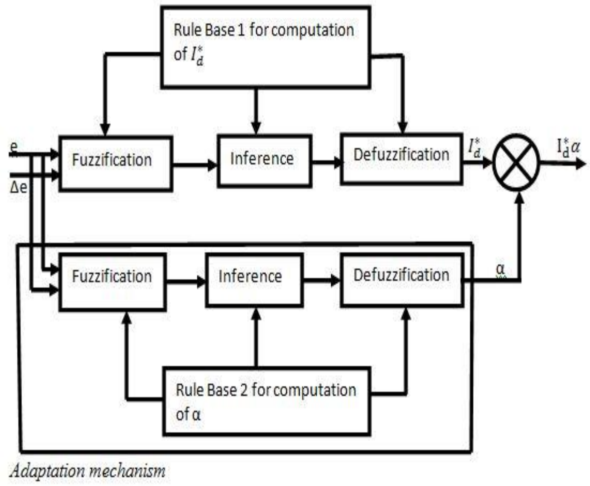

Fig. 10: AFLC Structure for GSC.

Table 3: Rule base for computation of α, α and γ

e / Δe	N	Z	P
N	NL	NM	Z
Z	NM	Z	PM
P	Z	PM	PL

Where N – Negative, PL- Positive Large ,P – Positive, NM – Negative Medium, PM – Positive Medium, NL- Negative Large, Z – Zero.

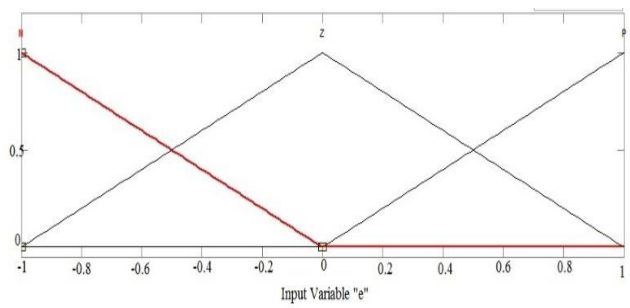

(a)

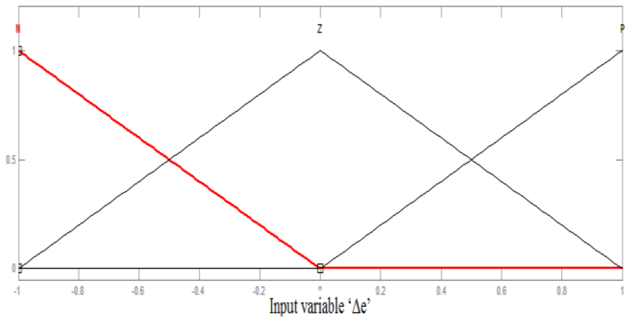

(b)

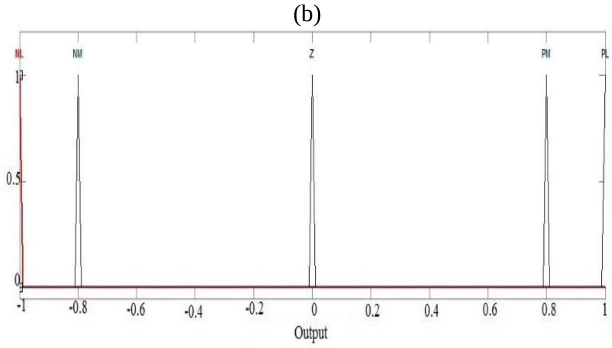

(c)

Fig .11: MF'S of AFLC for: (a) e (b)Δe and (c) output

6. Simulation results

The responses of the three controllers used, namely, PI, Fuzzy and AFLC are plotted.

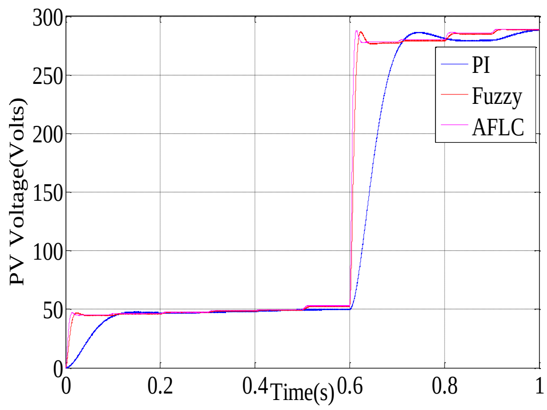

Fig.12: PV panel Output Voltage

Table .4: Comparison of t_r and t_s for PI, Fuzzy and AFLC

Controllers	t_r (sec)	t_s (sec)
PI	0.7	0.98
Fuzzy	0.62	0.89
AFLC	0.61	0.9

PV panel voltage for a change in PV panel irradiance input from 500W/m^2 to 1000W/m^2 from these results AFLC gives quick response compared to Fuzzy and PI which is shown in Fig.12.From table.4, AFLC has better tr and t_s compared to other two controllers.

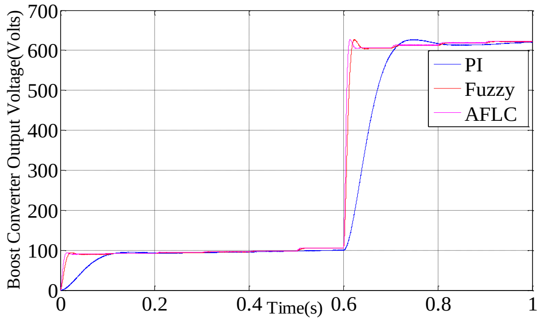

Fig.13: Boost converter output Voltage

Table 5: Comparison of t_r and t_s for PI, Fuzzy and AFLC

Controllers	t_r (sec)	t_s (sec)
PI	0.68	0.95
Fuzzy	0.62	0.92
AFLC	0.61	0.9

Boost converter output voltage for a change in solar panel voltage, when compared with PI and fuzzy, AFLC gives quick response which is shown in Fig.13.From table.5. AFLC has better tr and t_s compared to other two controllers.

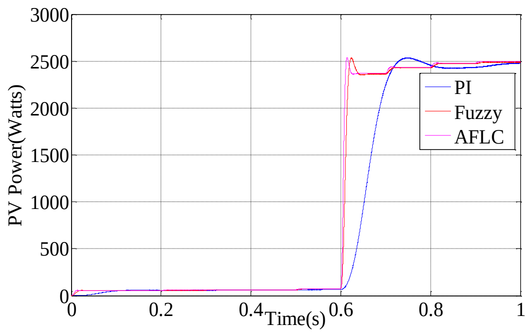

Fig.14: PV panel output power

Table 6: Comparison of $t_r$and t_s for PI, Fuzzy and AFLC controllers

Controllers	t_r (sec)	t_s (sec)
PI	0.7	0.98
Fuzzy	0.62	0.91
AFLC	0.61	0.89

PV Power, when compared with PI and fuzzy, AFLC give quick response which is shown in Fig.14. From table.6. AFLC has better t_r and t_s compared to other two controllers.

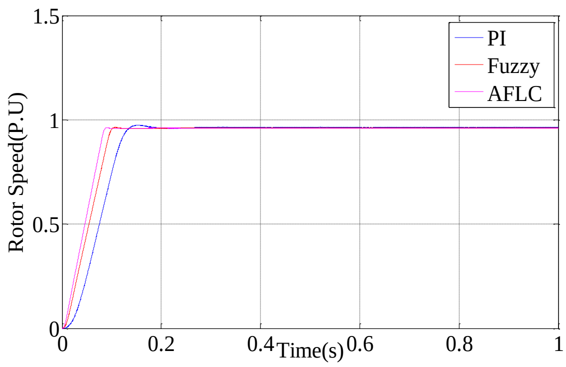

Fig.15: Rotor speed

Table 7: Comparison of t_r and t_s for PI, Fuzzy and AFLC controllers

Controllers	t_r (sec)	t_s (sec)
PI	0.15	0.2
Fuzzy	0.09	0.12
AFLC	0.08	0.09

From the table.7. Conclude that AFLC had better t_r and t_s compared to other two controllers.

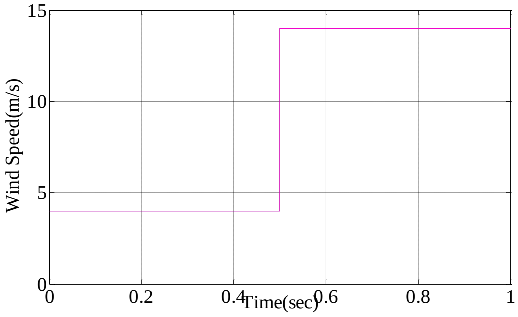

Fig.16: Wind speed

Simulation result for a period of 1sec with change in wind speed of 0.5 sec that is up to 0.5 sec 4 m/s after 0.5 sec 14 m/s shown in Fig.16.

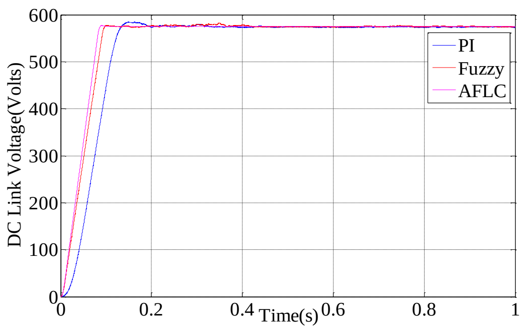

Fig.17: DC link voltage

Table 8: Comparison of t_r and t_s for PI, Fuzzy and AFLC controllers

Controllers	t_r (sec)	t_s (sec)
PI	0.13	0.25
Fuzzy	0.08	0.2
AFLC	0.07	0.09

From the table.8. Conclude that AFLC has better t_r and t_s compared to other two controllers. DC link voltage 580 V.

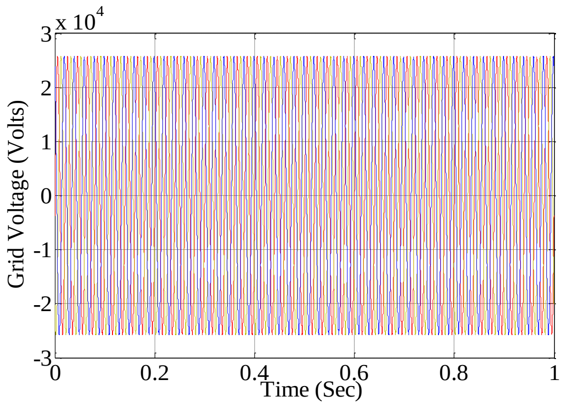

(a)

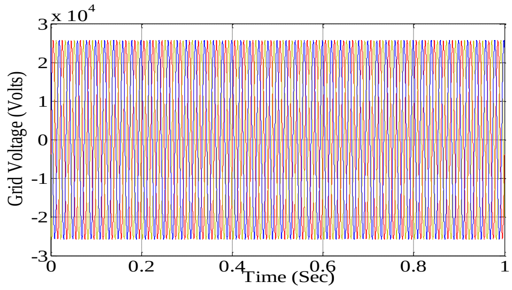

(b)

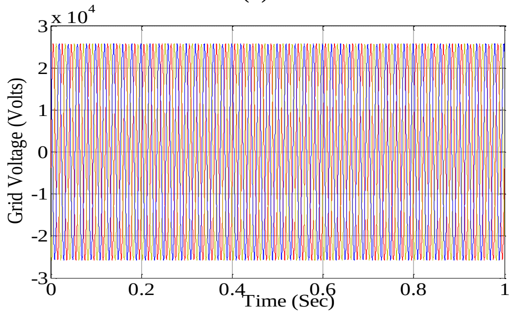

(c)

Fig.18: Simulation response of Grid Voltage with (a)PI (b) Fuzzy (c)AFLC

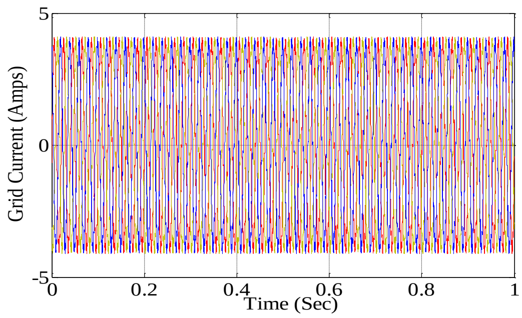

(a)

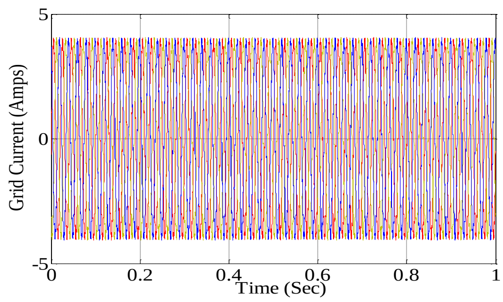

(b)

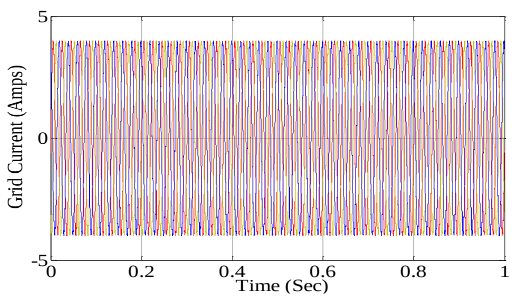

(c)

Fig. 19: Simulation response of Grid Current with (a)PI (b) Fuzzy (c)AFLC

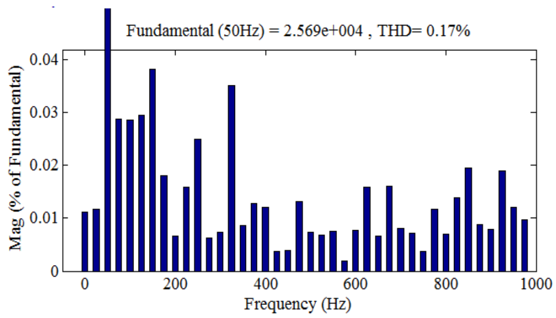

(a)

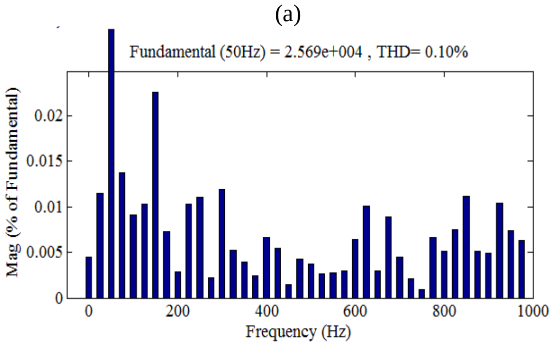

(b)

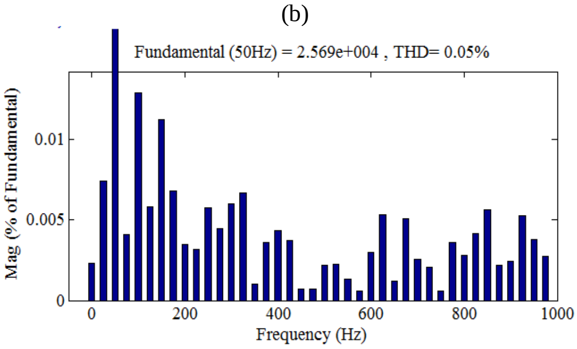

(c)

Fig. 20: THD of grid Voltage with (a)PI (b) fuzzy (c)AFLC

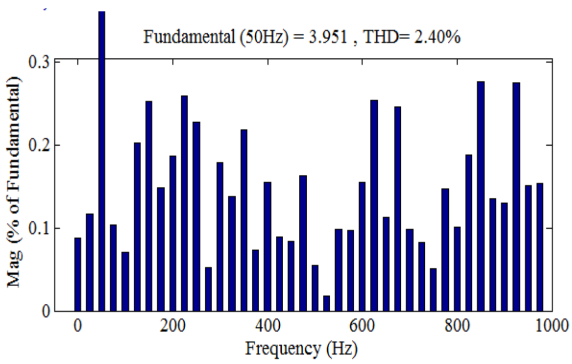

(a)

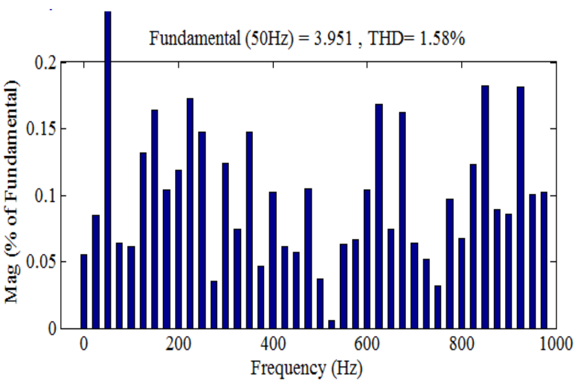

(b)

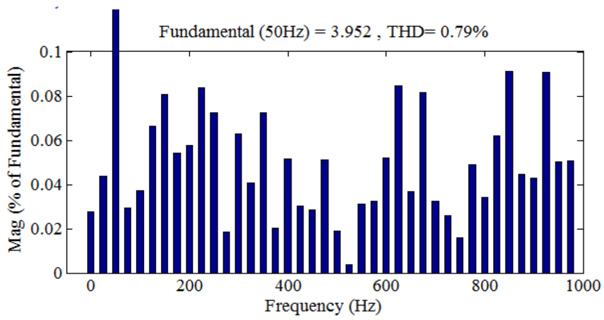

(c)

Fig.21: THD of grid current with (a)PI (b) Fuzzy (c)AFLC

THD of grid Current are better in AFLC compared to PI and Fuzzy controllers. From the Fig.21.

Table 9: Comparison performance between PI , Fuzzy and AFLC

S.No	Variable Name	PI Controller THD (%)	Fuzzy THD (%)	AFLC THD (%)
1	Grid Voltage	0.17	0.10	0.05
2	Grid current	2.40	1.58	0.79

The %THD value of AFLC is reduced by 50% approximately when compared to the PI and fuzzy THD values. From the table.9.It is observed that the AFLC gives better performance than the PI and fuzzy.

7. Conclusion

In this work, an AFLC is used to achieve fast response with change in wind speed. Simulation results show that the proposed AFLC controller gives fast response when compared with PI and fuzzy logic controller. From results it is observed that % THD for grid current and grid voltage are improved when AFLC is used.

References

[1]. Kuo-Yuan Lo, Yaow-Ming Chen, Senior Member, IEEE and Yung-Ruei Chang, Member, IEEE, "MPPT Battery Charger for Stand-Alone Wind Power System", IEEE Transactions On Power Electronics, Vol. 26, No 6, June 2011.

[2]. Rajesh K, A.D Kulkarni, T.Ananthapadmanbha " Modellingand SimulationofSolar PV and DFIG based Wind Hybrid System" Procedia Technology 21 (2015) 667-675.

[3]. Hussen,K.H., Murta.I., Hoshino.T., Osakada,M. "Maximum photovoltaic power tracking:an algorithm for rapidly changing atmosphericconditions",IEEE Proceedings of generation ,Transmission and Generation,vol.142,No.1,1995.

[4]. E.Koutroulis,et.AI, "Development of a Microcontroller-basedphotovoltaic maximum power tracking control system",IEEE Trans.on power Electron,Vol.16,No.1,2001,p.46-54.

[5]. R. Pena, J. C. Clare, and G. M. Asher, Doubly fed induction generatorusing back-to-back PWM converters and its application to variablespeed wind-energy generation, Proc. Inst. Elect. Eng., Elect. PowerAppl., vol. 143, no. 3, p. 231–241, May 1996

[6]. Nihel Khemiri, Adel Khedher, and Mohamed FaouziMimouni"Wind Energy Conversion System using DFIG Controlledby Backstepping and Sliding Mode Strategies''International journalof renewable energy research,Nihel Khemiri et al., Vol.2, No.3, 2012.

[7]. Abdelhak dida, djilani ben attous''doubly-fed inductiongenerator drive based WECS using fuzzy logic controller'' HigherEducation Press and Springer-Verlag Berlin Heidelberg 2015.

[8]. J.M. Carrasco, L.G. Franquelo, J.T. Bialasiewicz,E.Galván, R.C.P. Guisado, M.Á.M. Prats, J.I.León,andN.M.Alfonso, "Power-electronic systems for the gridintegration of renewable energy sources: A survey," *IEEE Trans. Ind. Electron.* vol. 53, no. 4, pp. 1002-1016, Aug. 2006.

[9]. [M.Azouz,A.shaltout and M.A.L.Elshafei’’Fuzzy logic control of wind energy systems” international middle East power systems conference december19-21,2010.
[10]. Aggarwal Archna,saini lalit mohan and singh bhim”control strategies for GFIG based grid connected wind energy conversion system” international journal of grid distribution computing vol.7.no.3(2014)pp49-60.
[11]. Abdelhak DIDA, Djilani BEN ATTOUS” Doubly- fed induction generator drive based WECS using fuzzy logic controller” Springer-Verlag Berlin Heidelberg,2015.
[12]. C.Sudhakar,P.Bharat Kumar, “ANFIS approach based on MPPT for multi intersection solar cell PV Energy”,JARDCS,Vol.9,pp.1349-1362,2017.
[13]. R. Kalaivani, K. Ramash Kumar, S. Jeevananthan, “Implementation of VSBSMC plus PDIC for Fundamental Positive Output Super Lift-Luo Converter,” Journal of Electrical Engineering, Vol. 16, Edition: 4, 2016, pp. 243-258.
[14]. K. Ramash Kumar,”Implementation of Sliding Mode Controller plus Proportional Integral Controller for Negative Output Elementary Boost Converter,” Alexandria Engineering Journal (Elsevier), 2016, Vol. 55, No. 2, pp. 1429-1445.
[15]. P. Sivakumar, V. Rajasekaran, K. Ramash Kumar, “Investigation of Intelligent Controllers for Varibale Speeed PFC Buck-Boost Rectifier Fed BLDC Motor Drive,” Journal of Electrical Engineering (Romania), Vol.17, No.4, 2017, pp. 459-471.
[16]. K. Ramash Kumar, D.Kalyankumar, DR.V.Kirbakaran” An Hybrid Multi level Inverter Based DSTATCOM Control, Majlesi Journal of Electrical Engineering, Vol. 5. No. 2, pp. 17-22, June 2011, ISSN: 0000-0388.
[17]. K. Ramash Kumar, S. Jeevananthan, “A Sliding Mode Control for Positive Output Elementary Luo Converter,” Journal of Electrical Engineering, Volume 10/4, December 2010, pp. 115-127.
[18]. K. Ramash Kumar, Dr.S. Jeevananthan,” Design of a Hybrid Posicast Control for a DC-DC Boost Converter Operated in Continuous Conduction Mode” (IEEE-conference PROCEEDINGS OF ICETECT 2011), pp-240-248, 978-1-4244-7925-2/11.